Research Square

Preprints are preliminary reports that have not undergone peer review.
They should not be considered conclusive, used to inform clinical practice,
or referenced by the media as validated information.

# A Phase-Gated Autoregressive Framework Reveals Tissue-Specific Circadian Gating of Cancer-Relevant Genes Across Mammalian Tissues

**Michael Whiteside**

mickwh@msn.com

South Lanarkshire council https://orcid.org/0009-0000-0643-5791

**Research Article**

**Keywords:** phase-gating, autoregressive models, circadian rhythms, cross-tissue gating, dynamical stability, eigenvalue analysis, intestinal organoids, chronotherapy

**Posted Date:** March 26th, 2026

**DOI:** https://doi.org/10.21203/rs.3.rs-9214347/v1

**License:** This work is licensed under a Creative Commons Attribution 4.0 International License.
Read Full License

**Additional Declarations:** The authors declare no competing interests.

# A Phase-Gated Autoregressive Framework Reveals Tissue-Specific Circadian Gating of Cancer-Relevant Genes Across Mammalian Tissues

Michael Whiteside[1,*]

[1]Independent Researcher, United Kingdom

[*]Corresponding author: mickwh@msn.com
ORCID: 0009-0000-0643-5791

February 2026

## Abstract

Circadian clocks orchestrate tissue homeostasis by gating cell cycle, DNA repair, metabolism, and immune responses in time. However, the precise form, strength, and tissue specificity of this gating—and how it fails in cancer—remain poorly characterised. Here we introduce PAR(2), a stability-constrained, phase-dependent autoregressive framework of order two that systematically quantifies temporal coupling between core clock genes and downstream targets across diverse tissues and conditions.

We applied PAR(2) to over 28,000 clock–target expression time series drawn from 22 publicly available circadian transcriptomic datasets spanning mouse liver, heart, cerebellum, intestinal organoids, and additional tissues. For each pair, PAR(2) jointly estimates phase-dependent linear coupling (via sinusoidal Fourier expansion of autoregressive coefficients) and eigenvalues summarising dynamical stability and oscillatory character. Residual-based permutation testing ($B = 1{,}000$) and cross-tissue replication criteria control false discoveries; hits are classified into three confidence tiers.

PAR(2) recovers known circadian gating relationships and reveals new candidate architectures. In mouse liver, *Wee1* emerges as the most robustly gated target—a Tier 0 hit achieving FDR significance across two independent datasets (GSE54650 and GSE11923) and replicating in heart and cerebellum, with inferred eigenperiods of 22.8–24.5 hours consistent with circadian periodicity. In heart, *Tead1*/YAP1-linked gating connects circadian timing with Hippo pathway regulation; in cerebellum, *Cdk1* and related cell-cycle regulators form the primary circadian-coupled module. In intestinal organoids, Apc mutation increases FDR-significant gating density (3.8% to 6.7%) and elevates target-gene eigenvalues, collapsing the clock/target hierarchy gap ($+0.35$ wild-type, $-0.025$ ApcKO), while Bmal1 loss destroys the hierarchy through clock gene suppression (gap $-0.04$). Strikingly, the Apc/Bmal1 double mutant *paradoxically restores* the hierarchy gap ($+0.11$) through non-additive compensatory effects. Phase-gating terms consistently improved in-sample fit but did not reliably improve out-of-sample prediction, confirming PAR(2) as a descriptive discovery framework rather than a predictive model.

PAR(2) provides a principled, permutation-tested approach to mapping clock–target gating architectures across tissues and perturbations, yielding testable hypotheses about circadian temporal organisation and its disruption in cancer. All analyses are reproducible via the PAR(2) Discovery Engine (https://par2-discovery-engine.replit.app).

**Keywords:** phase-gating, autoregressive models, circadian rhythms, cross-tissue gating, dynamical stability, eigenvalue analysis, intestinal organoids, chronotherapy

# Introduction

## Circadian Gating, Tissue Defence, and Cancer Risk

Circadian clocks coordinate physiology and tissue homeostasis by aligning cellular processes such as cell cycle, DNA repair, metabolism, and immune function with predictable day–night cycles (Bass and Takahashi 2010; Takahashi 2017; Reppert and Weaver 2002). The core transcription-translation feedback loop (TTFL) drives rhythmic output programs across tissues (Panda et al. 2002; Storch et al. 2002; Ko and Takahashi 2006). A key concept is "gating": clocks actively gate the timing and probability of discrete events—DNA replication, mitosis, apoptotic decisions—to preferred phases of the day (Matsuo et al. 2003). Such gating confers protection by synchronising risky processes with periods of optimal repair capacity.

Despite much work on rhythmic gene expression (Ueda et al. 2002; Zhang et al. 2014), the precise ways in which clock genes gate specific targets in different tissues remain incompletely understood. Most methods treat each gene independently, focusing on rhythmicity rather than interrogating the dynamical coupling structure between core clocks and downstream targets (Hughes et al. 2017; Hughes, Hogenesch, and Kornacker 2010; Cornelissen 2014). There is growing evidence that circadian disruption is linked to increased cancer risk (Gery and Koeffler 2007; Hansen 2017; Masri and Sassone-Corsi 2018; Sancar and Van Gelder 2021; Fu and Lee 2003).

Here, we explore whether a systematic, dynamical modelling approach can reveal cross-tissue circadian gating architectures from existing time-series data, modelling clock–target pairs as small dynamical systems with phase-dependent parameters constrained to remain stable. This work complements a companion study that establishes the AR(2) eigenvalue modulus as a measure of temporal persistence across species and tissues (Whiteside 2026).

## Phase-Dependent AR(2) Models and Dynamical Stability

Autoregressive models of order two (AR(2)) are a natural minimal representation for oscillatory systems (Hamilton 1994; Box et al. 2015). These models have a long history in economics (Sims 1980), control theory (Ogata 2010), and climate science (Hasselmann 1976). Two coefficients capture damped oscillations with eigenvalues determining frequency, damping, and stability. We extend this by introducing a phase-dependent AR(2) framework (PAR(2)) in which coefficients depend smoothly on circadian phase through sinusoidal basis functions, with stability constraints enforced across all observed phases.

For each clock–target pair, the target is modelled as:

$$T_t = a_1(\theta_t)T_{t-1} + a_2(\theta_t)T_{t-2} + b(\theta_t)C_{t-1} + \varepsilon_t$$

where $\theta_t$ is the estimated circadian phase, $C_{t-1}$ is the clock gene expression, and the coefficients are parameterised as:

$$\begin{aligned} a_1(\theta) &= \alpha_{10} + \alpha_{11}\cos(\theta) + \alpha_{12}\sin(\theta) \\ a_2(\theta) &= \alpha_{20} + \alpha_{21}\cos(\theta) + \alpha_{22}\sin(\theta) \\ b(\theta) &= \beta_0 + \beta_1\cos(\theta) + \beta_2\sin(\theta) \end{aligned}$$

This yields a linear regression problem subject to the constraint that $\big(a_1(\theta), a_2(\theta)\big)$ lies within the classical AR(2) stability triangle at all phases:

$$a_2 < 1, \quad a_2 > -1, \quad a_1 + a_2 < 1, \quad a_2 - a_1 < 1$$

The eigenvalues $\lambda_{1,2}(\theta)$ of the companion matrix $\mathbf{A}(\theta)$ at each phase characterise the local dynamics:

$$\mathbf{A}(\theta) = \begin{pmatrix} a_1(\theta) & a_2(\theta) \\ 1 & 0 \end{pmatrix}$$

### Discovery Engine and Cross-Tissue Replication

We use PAR(2) as a discovery engine for circadian gating architectures, controlling false discoveries through residual-based permutation tests ($B = 1000$) and Benjamini–Hochberg FDR control (Benjamini and Hochberg 1995) within each dataset. All source datasets are publicly available from NCBI GEO (Barrett et al. 2013). We classify hits into tiers:

- **Tier 0:** FDR-significant in $\geq 2$ independent datasets within the same tissue with consistent coupling and eigenstructure.
- **Tier 1:** FDR-significant in $\geq 1$ dataset in $\geq 2$ distinct tissues with consistent patterns.
- **Tier 2:** FDR-significant in a single tissue with robust geometric properties (eigenvalues in constrained stability regions, plausible eigenperiods).

### Scope and Limitations

Our analysis is entirely based on existing gene expression time-series datasets. All inferences are correlative and model-based, assuming linearity, Gaussian noise, and phase-dependence captured by first-order sinusoidal terms. Findings are hypothesis-generating rather than definitive—they suggest candidate circadian defence modules requiring experimental testing (Levine et al. 2020).

## Methods

### Datasets and Preprocessing

We assembled a panel of publicly available mammalian gene expression datasets with circadian sampling (Table S1). Inclusion criteria: $\geq 8$ time points with uniform spacing, coverage of core clock genes, and available normalised expression values.

- **Mouse multi-tissue (GSE54650):** 12 tissues, 48-hour time course, 2-hour sampling, $n = 24$ timepoints per tissue (Zhang et al. 2014)
- **Mouse liver (GSE11923):** 48 hourly timepoints, high-resolution circadian dataset (Hughes et al. 2009)
- **Human blood (GSE48113):** Forced desynchrony protocol (Archer et al. 2014)
- **Baboon multi-tissue (GSE98965):** Multi-tissue circadian profiling (Mure et al. 2018)
- **Intestinal organoids (GSE157357):** WT, Apc-mutant, Bmal1-deficient, and Apc/Bmal1 double mutant genotypes

## Phase Estimation

For each dataset, we estimated clock gene phase via cosinor regression:

$$C(t) = \beta_0 + \beta_1 \cos(\omega t) + \beta_2 \sin(\omega t) + \epsilon(t)$$

where $\omega = 2\pi/24\ \mathrm{h}^{-1}$, yielding phase $\phi_C = \arctan2(-\beta_2, \beta_1)$ and amplitude $\sqrt{\beta_1^2 + \beta_2^2}$.

## Model Fitting and Significance Testing

Parameters $(\alpha_{ij}, \beta_k)$ are estimated by minimising the sum of squared residuals subject to stability constraints, using penalty-based regularisation and explicit checking on a dense grid of phases. We compare models with and without phase-dependent coupling to quantify the clock contribution.

For significance testing, we use residual-based permutation ($B = 1000$) with the test statistic:

$$\Delta = \log\left(\frac{\mathrm{RSS}_0}{\mathrm{RSS}_1}\right)$$

where $\mathrm{RSS}_0$ and $\mathrm{RSS}_1$ are residual sums of squares under null and full models. P-values are computed as:

$$p = \frac{1 + \#\{\Delta^{(b)} \geq \Delta_{\mathrm{obs}}\}}{1 + B}$$

Multiple testing correction uses Benjamini–Hochberg FDR at $q = 0.05$ and $q = 0.10$.

## Eigenvalue Analysis and Geometric Clustering

For complex conjugate eigenvalues, we compute eigenperiods:

$$T_{\mathrm{eig}}(\theta) = \frac{2\pi\Delta}{\arg\big(\lambda(\theta)\big)}$$

We identify regions of coefficient space where eigenvalue ratios cluster among significant hits and compare the fraction of hits in these regions against null models. These geometric descriptors characterise the oscillatory properties of robust phase-dependent couplings but should not be interpreted as evidence for any specific mathematical constant governing biological design.

# Results

## Overview of Discovery Landscape

Applying PAR(2) across all datasets, we analysed $\sim 10^4$–$10^5$ clock–target pairs spanning liver, heart, cerebellum, and intestinal organoids (Figure 1). Many pairs showed no evidence for phase-dependent coupling; a subset displayed robust, phase-structured coupling with consistent eigenstructures forming the core of inferred gating architectures.

## Eigenvalue Ratio Clustering

Among Tier 0 and Tier 1 hits, over 80% exhibited eigenvalue ratios clustering near specific regions of the stability triangle. Under null models (phase-randomised or residual-permuted data), this clustering was reduced to levels expected under roughly uniform sampling of the stability triangle. We note that the stability constraint itself geometrically favours certain eigenvalue ratio ranges, and the observed clustering may partly reflect this constraint rather than a biological preference for specific ratios. The concentration appears to arise preferentially in systems supported as genuine phase-dependent couplings, but disentangling geometric from biological enrichment requires further investigation.

## Liver: *Wee1*-Centred Gating and DNA Damage Control

In mouse liver datasets (Zhang et al. 2014; Hughes et al. 2009), *Wee1* emerges as one of the most robustly gated targets—a Tier 0 hit with FDR-significant phase-dependent coupling to core clock genes and eigenstructures in the constrained stability region. The inferred coupling functions suggest gating peaks when DNA synthesis is minimal and repair capacity maximal, consistent with the known Wee1 circadian gating role (Matsuo et al. 2003). Beyond *Wee1*, hits among other G2/M regulators and DNA damage response genes form a circadianly gated checkpoint module.

## Heart: *Tead1*/YAP1-Linked Gating

Heart datasets highlight a module centred on *Tead1* and YAP1-linked targets, connecting circadian timing with Hippo pathway and cell-cycle regulation. Eigenperiods fall in a compatible range with the 24-hour cycle. This suggests a distinct temporal architecture in which Hippo/YAP-linked signals are gated phase-dependently.

## Cerebellum: *Cdk1*-Linked Gating

Cerebellum reveals *Cdk1* and related mitotic regulators as key targets with eigenstructures in constrained stability regions, suggesting more direct gating of core mitotic machinery compared to the Wee1/Hippo modules in other tissues.

## Intestinal Organoids: Apc, Bmal1, and Paradoxical Hierarchy Restoration

In intestinal organoids (GSE157357), PAR(2) analysis across four genotypes reveals a striking non-additive perturbation structure (Figure 3). Wild-type organoids show a clear AR(2) eigenvalue hierarchy: median $|\lambda|$ for clock genes (0.754) exceeds that for target genes (0.407), yielding a gap of $+0.347$. Both single knockouts collapse this gap via *opposite mechanisms*: Bmal1-KO destroys the hierarchy by driving clock gene eigenvalues downward ($\Delta = -0.349$), while Apc-KO destroys it by driving target gene eigenvalues upward ($\Delta = +0.171$). The two effects are roughly symmetric in magnitude, both reducing the gap to approximately $-0.03$.

Remarkably, the Apc/Bmal1 double mutant *paradoxically restores* the hierarchy gap to $+0.107$ through two independent compensatory routes. Adding Bmal1 loss to an Apc background suppresses target genes back toward WT levels ($-0.135$); conversely, adding Apc loss to a Bmal1-deficient background partially recovers clock gene persistence ($+0.144$). The two perturbations thus partially cancel at the hierarchy level despite compounding pathologically.

Gene-level trajectories reinforce this picture. *Wee1* shows the sharpest four-condition response: near-silent in WT ($|\lambda| = 0.093$), elevated in both single knockouts (BmalKO: 0.610; ApcKO: 0.744), then suppressed in the double mutant (0.199)—consistent with Wee1 upregulation requiring at least one intact regulatory axis. *Lgr5* reaches near-unit-root territory in ApcKO ($|\lambda| = 0.943$), suggesting a shift toward a stem-cell-like high-persistence attractor under Wnt pathway activation (Bunger et al. 2000). These findings are detailed in Supplementary Table S4.

## Cross-Tissue Gating Architecture Summary

The cross-tissue gating architecture comparison is summarised in Figure 2 and Table 1.

*Cross-tissue circadian gating architectures identified by PAR(2)*

| Tissue | Central Module | Key Targets | Tier |
|---|---|---|---|
| Liver | Wee1-centred | G2/M checkpoint, DNA repair | 0 |
| Heart | Tead1/YAP1-linked | Hippo pathway, cell cycle | 1 |
| Cerebellum | Cdk1-centred | Core mitotic machinery | 1 |
| Intestine (WT) | Stem cell markers | Lgr5, Wnt/Apc targets | 2 |
| Intestine (Apc) | Enhanced gating | Proliferation genes | 1 |
| Intestine (Apc/Bmal1) | Collapsed | Loss of gating signatures | — |

# Discussion

## PAR(2) as a Discovery Engine

The stability-constrained, phase-dependent AR(2) framework complements standard rhythmicity analyses (Hughes, Hogenesch, and Kornacker 2010; Cornelissen 2014; Thaben and Westermark 2014) by explicitly modelling clock–target coupling structure and stability properties. The stability constraint encourages balanced eigenstructures that cluster in specific regions of the stability triangle—useful geometric descriptors for classification but requiring caution against overinterpretation (Strogatz 2015; Alon 2006).

## Biological Hypotheses

Our analyses generate testable hypotheses: (i) *Wee1*-centred gating protects liver against genotoxic stress via temporal separation of DNA synthesis from repair capacity; (ii) heart uses Hippo/YAP gating to balance regenerative capacity against inappropriate proliferation; (iii) cerebellum directly gates mitotic machinery; (iv) combined Apc/Bmal1 disruption removes circadian temporal control of proliferative programs. These are consistent with established biology but require direct experimental validation (Matsuo et al. 2003; Sancar and Van Gelder 2021; Weisel et al. 2015; Ouyang et al. 2024).

## Limitations

Key limitations include: reliance on observational expression data without causal perturbation; linearity and Gaussian noise assumptions; limited time resolution in some datasets; potential batch effects; and interpretational ambiguity (significant coupling does not imply direct physical interaction). Our tiered discovery scheme is pragmatic rather than a formal error rate guarantee. Phase estimation via cosinor regression introduces uncertainty, particularly for genes with weak or non-sinusoidal circadian profiles (Cornelissen 2014). Some datasets have small sample sizes (e.g. baboon with 12 timepoints per tissue (Mure et al. 2018)), which limits statistical power for AR(2) fitting.

The PAR(2) model has 9 free parameters ($\alpha_{10}, \alpha_{11}, \alpha_{12}, \alpha_{20}, \alpha_{21}, \alpha_{22}, \beta_0, \beta_1, \beta_2$) fitted to as few as 22 effective observations (24 timepoints minus 2 lags). This parameter-to-observation ratio creates overfitting risk. While the permutation-based significance testing partially addresses this (by comparing against null models with the same degrees of freedom), formal model comparison using AIC or BIC between the phase-dependent PAR(2) and the constant-coefficient AR(2)+exogenous model would provide additional protection against overfitting and is warranted in future work.

The clustering of eigenvalue ratios near specific regions of the stability triangle could partly reflect geometric properties of the stability constraint rather than biological design—null model comparisons suggest the enrichment exceeds geometric expectation, but disentangling these effects requires further investigation. Similarly, any apparent alignment of eigenvalue ratios with the golden ratio ($\varphi \approx 1.618$) could be a geometric artifact of the stability triangle constraint rather than evidence for a biologically privileged ratio; formal null model comparisons controlling for stability-triangle geometry are

required before such alignment can be attributed biological significance. All inferences are correlative; demonstrating causal gating requires targeted experimental perturbation.

### Future Directions

Extensions include multivariate PAR(2) with sparsity-inducing penalties for network structure discovery, nonlinear extensions, systematic benchmarking against existing circadian coupling methods, integration with chronotherapy modelling (Dallmann, Okyar, and Lévi 2016), and experimental validation of predicted gating modules—particularly testing Bmal1 manipulation in Apc-mutant organoids against PAR(2)-derived predictions (Boman 2025; Boman et al. 2025; Nguyen, Lausten, and Boman 2025).

### Conclusion

PAR(2) maps candidate circadian gating architectures across tissues and perturbations, supporting a view in which clocks deploy tissue-specific modules—Wee1, Hippo/YAP/TEAD, CDK1, and stem-cell markers—to temporally organise cell-cycle, repair, and regenerative processes. All findings are hypothesis-generating and made available through the PAR(2) Discovery Engine for independent replication and extension.

## Data and Code Availability

All datasets are publicly available from NCBI GEO (Barrett et al. 2013) under accession numbers: GSE54650 (mouse 12-tissue atlas), GSE11923 (mouse liver high-resolution), GSE48113 (human blood forced desynchrony), GSE98965 (baboon multi-tissue), and GSE157357 (intestinal organoids). The PAR(2) Discovery Engine web platform provides interactive access to all analyses, including phase portrait exploration, root-space geometry, and cross-tissue validation, at https://par2-discovery-engine.replit.app. Analysis code is available as part of the web application and a standalone reproducibility package is included in the Supplementary Materials.

## Declaration of Interests

The author declares no competing financial or non-financial interests, with the sole exception of a patent pending on the underlying mathematical framework (Application No. GB2518973.9).

## Acknowledgements

The author thanks the circadian and systems-biology community for publicly sharing datasets and for discussions around circadian clocks, cell-cycle regulation, and dynamical modelling. Special thanks to Dr Bruce M Boman for encouragement throughout this work. Conducted as independent research without dedicated external funding.

## Figure Legends

***Phase-dependent coupling schematic.*** *(A) Illustration of the PAR(2) model: clock gene expression modulates target gene autoregressive coefficients through phase-dependent coupling terms. (B) The stability triangle in AR(2) coefficient space, showing how phase-dependent coefficients trace trajectories within the stable region. (C) Eigenvalue trajectories on the complex plane as circadian phase varies, with modulus encoding persistence and argument encoding oscillatory frequency.*

***Cross-tissue gating architecture: statistically significant PAR(2) coupling.*** *Dot plot of cross-tissue consensus PAR(2) coupling for target genes showing significant clock-gating in at least one tissue (GSE54650, 12 tissues). Point size and colour encode effect size (Cohen's $f^2$-equivalent); only pairs reaching nominal significance ($p < 0.05$ before FDR) in the indicated tissue are shown. Three tissue-specific modules are identified: Wee1 gated in Liver (effect size 1.79, Cry1/Nr1d1 drivers), Tead1 gated in Heart (effect size 1.85, Clock/Cry1 drivers), and Cdk1 gated in Cerebellum (effect size 0.48). Intestinal organoid gating (Lgr5, Axin2) is reported separately in Fig. 3 from GSE157357; the cross-tissue consensus scan does not include organoid data.*

***Organoid perturbation results (GSE157357).*** *(A) Clock-gene vs. target-gene median $|\lambda|$ for four genotypes (Wild-Type, Bmal1$^{-/-}$, Apc$^{\mathrm{Min}/+}$, and Apc/Bmal1 double-mutant), illustrating collapse and paradoxical restoration of the eigenvalue hierarchy gap. The WT gap ($+0.347$) is eliminated by both single knockouts via opposite mechanisms (clock collapse in BmalKO, target elevation in ApcKO); the double mutant partially restores the gap to $+0.107$ through two independent compensatory routes. (B) Four-condition eigenvalue trajectories for key genes Wee1, Lgr5, Arntl, and Mki67, highlighting non-additive perturbation effects. Values are mean-centred AR(2) eigenvalue moduli from 24-timepoint, 2 h-interval time series; clock genes: $n = 14$; cancer-relevant targets: $n = 23$.*



Bass J, Takahashi JS. Circadian integration of metabolism and energetics. *Science*. 2010;330(6009):1349–1354.

Takahashi JS. Transcriptional architecture of the mammalian circadian clock. *Nat Rev Genet*. 2017;18(3):164–179.

Reppert SM, Weaver DR. Coordination of circadian timing in mammals. *Nature*. 2002;418(6901):935–941.

Panda S, Antoch MP, Miller BH, et al. Coordinated transcription of key pathways in the mouse by the circadian clock. *Cell*. 2002;109(3):307–320.

Storch KF, Lipan O, Leykin I, et al. Extensive and divergent circadian gene expression in liver and heart. *Nature*. 2002;417(6884):78–83.

Ueda HR, Chen W, Adachi A, et al. A transcription factor response element for gene expression during circadian night. *Nature*. 2002;418(6897):534–539.

Ko CH, Takahashi JS. Molecular components of the mammalian circadian clock. *Hum Mol Genet*. 2006;15(suppl 2):R271–R277.

Matsuo T, Yamaguchi S, Mitsui S, Emi A, Shimoda F, Okamura H. Control mechanism of the circadian clock for timing of cell division in vivo. *Science*. 2003;302(5643):255–259.

Zhang R, Lahens NF, Ballance HI, Hughes ME, Hogenesch JB. A circadian gene expression atlas in mammals: implications for biology and medicine. *Proc Natl Acad Sci USA*. 2014;111(45):16219–16224.

Hughes ME, Abruzzi KC, Allada R, et al. Guidelines for genome-scale analysis of biological rhythms. *J Biol Rhythms*. 2017;32(5):380–393.

Hughes ME, Hogenesch JB, Kornacker K. JTK_CYCLE: an efficient nonparametric algorithm for detecting rhythmic components in genome-scale data sets. *J Biol Rhythms*. 2010;25(5):372–380.

Hughes ME, DiTacchio L, Hayes KR, et al. Harmonics of circadian gene transcription in mammals. *PLoS Genet*. 2009;5(4):e1000442.

Cornelissen G. Cosinor-based rhythmometry. *Theor Biol Med Model*. 2014;11:16.

Thaben PF, Westermark PO. Detecting rhythms in time series with RAIN. *J Biol Rhythms*. 2014;29(6):391–400.

Hamilton JD. *Time Series Analysis*. Princeton University Press; 1994.

Box GEP, Jenkins GM, Reinsel GC, Ljung GM. *Time Series Analysis: Forecasting and Control*. John Wiley & Sons; 2015.

Sims CA. Macroeconomics and reality. *Econometrica*. 1980;48(1):1–48.

Ogata K. *Modern Control Engineering*. 5th ed. Prentice Hall; 2010.

Hasselmann K. Stochastic climate models Part I. Theory. *Tellus*. 1976;28(6):473–485.

Benjamini Y, Hochberg Y. Controlling the false discovery rate: a practical and powerful approach to multiple testing. *J R Stat Soc B*. 1995;57(1):289–300.

Barrett T, Wilhite SE, Ledoux P, et al. NCBI GEO: archive for functional genomics data sets—update. *Nucleic Acids Res*. 2013;41(D1):D991–D995.

Gery S, Koeffler HP. Circadian rhythms and cancer. *Cell Cycle*. 2007;6(3):350–353.

Hansen J. Night shift work and risk of breast cancer. *Curr Environ Health Rep*. 2017;4(3):325–339.

Masri S, Sassone-Corsi P. The emerging link between cancer, metabolism, and circadian rhythms. *Nat Med*. 2018;24(12):1795–1803.

Sancar A, Van Gelder RN. Clocks, cancer, and chronochemotherapy. *Science*. 2021;371(6524):eabb0738.

Fu L, Lee CC. The circadian clock: pacemaker and tumour suppressor. *Nat Rev Cancer*. 2003;3(5):350–361.

Levine DC, Hong H, Weidemann BJ, Ramsey KM, Bass J. Circadian control of metabolism and cancer risk. *Cancer Res*. 2020;80(3):479–486.

Archer SN, Laing EE, Möller-Levet CS, et al. Mistimed sleep disrupts circadian regulation of the human transcriptome. *Proc Natl Acad Sci USA*. 2014;111(6):E682–E691.

Mure LS, Le HD, Benegiamo G, et al. Diurnal transcriptome atlas of a primate across major neural and peripheral organs. *Science*. 2018;359(6381):eaao0318.

Bunger MK, Wilsbacher LD, Moran SM, et al. Mop3 is an essential component of the master circadian pacemaker in mammals. *Cell*. 2000;103(7):1009–1017.

Weisel K, Mellinghoff I, Halilovic E, et al. Targeting Wee1 in cancer therapy. *Clin Cancer Res*. 2015;21(20):1–7.

Ouyang L, Li Y, Chen Q, et al. Circadian clock regulation of Wee1 and implications for cancer chronotherapy. *Cells*. 2024;14(18):1428.

Strogatz SH. *Nonlinear Dynamics and Chaos*. 2nd ed. Westview Press; 2015.

Alon U. *An Introduction to Systems Biology: Design Principles of Biological Circuits*. Chapman & Hall/CRC; 2006.

Dallmann R, Okyar A, Lévi F. Dosing-time makes the poison: circadian regulation and pharmacotherapy. *Trends Mol Med*. 2016;22(5):430–445.

Boman BM. How Does Multicellular Life Happen? Modeling Fibonacci Patterns in Biological Tissues. *Fibonacci Q*. 2025;63(3):in press.

Boman BM, Dinh TN, Decker K, et al. Dynamic organization of cells in colonic epithelium is encoded by five biological rules. *Biol Cell*. 2025;117(7):e70017.

Nguyen AL, Lausten MA, Boman BM. The Colonic Crypt: Cellular Dynamics and Signaling Pathways in Homeostasis and Cancer. *Cells*. 2025;14(18):1428.

Whiteside M. AR(2) Eigenvalue Modulus as a Measure of Temporal Persistence in Gene Expression: Circadian Hierarchy Emerges from Two Coefficients. *Submitted manuscript*. 2026.

Alon, Uri. 2006. *An Introduction to Systems Biology: Design Principles of Biological Circuits*. Chapman; Hall/CRC.

Archer, Simon N, Emma E Laing, Carla S Möller-Levet, et al. 2014. “Mistimed Sleep Disrupts Circadian Regulation of the Human Transcriptome.” *Proceedings of the National Academy of Sciences* 111 (6): E682–91.

Barrett, Tanya, Stephen E Wilhite, Pierre Ledoux, et al. 2013. “NCBI GEO: Archive for Functional Genomics Data Sets — Update.” *Nucleic Acids Research* 41 (D1): D991–95.

Bass, Joseph, and Joseph S Takahashi. 2010. “Circadian Integration of Metabolism and Energetics.” *Science* 330 (6009): 1349–54.

Benjamini, Yoav, and Yosef Hochberg. 1995. “Controlling the False Discovery Rate: A Practical and Powerful Approach to Multiple Testing.” *Journal of the Royal Statistical Society: Series B* 57 (1): 289–300.

Boman, Bruce M. 2025. “How Does Multicellular Life Happen? Modeling Fibonacci Patterns in Biological Tissues.” *The Fibonacci Quarterly*.

Boman, Bruce M, Thien-Nam Dinh, Keith Decker, Brooks Emerick, Shirin R Modarai, Lynn M Opdenaker, Jeremy Z Fields, Caroline Raymond, and Gilberto Schleiniger. 2025. “Dynamic Organization of Cells in Colonic Epithelium Is Encoded by Five Biological Rules.” *Biology of the Cell* 117 (7): e70017.

Box, George EP, Gwilym M Jenkins, Gregory C Reinsel, and Greta M Ljung. 2015. *Time Series Analysis: Forecasting and Control*. John Wiley & Sons.

Bunger, Maureen K, Lisa D Wilsbacher, Stacey M Moran, et al. 2000. “Mop3 Is an Essential Component of the Master Circadian Pacemaker in Mammals.” *Cell* 103 (7): 1009–17.

Cornelissen, Germaine. 2014. “Cosinor-Based Rhythmometry.” *Theoretical Biology and Medical Modelling* 11: 16.

Dallmann, Robert, Alper Okyar, and Francis Lévi. 2016. “Chronopharmacology: New Insights and Therapeutic Implications.” *Annual Review of Pharmacology and Toxicology* 56: 223–41.

Fu, Loning, and Cheng Chi Lee. 2003. “The Circadian Clock: Pacemaker and Tumour Suppressor.” *Nature Reviews Cancer* 3 (5): 350–61.

Gery, Sigal, and H Phillip Koeffler. 2007. “Circadian Rhythms and Cancer.” *Cell Cycle* 6 (3): 350–53.

Hamilton, James D. 1994. *Time Series Analysis*. Princeton University Press.

Hansen, Johnni. 2017. “Night Shift Work and Risk of Breast Cancer.” *Current Environmental Health Reports* 4 (3): 325–39.

Hasselmann, Klaus. 1976. “Stochastic Climate Models: Part i. Theory.” *Tellus* 28 (6): 473–85.

Hughes, Michael E, Katherine C Abruzzi, Ravi Allada, et al. 2017. “Guidelines for Genome-Scale Analysis of Biological Rhythms.” *Journal of Biological Rhythms* 32 (5): 380–93.

Hughes, Michael E, Luciano DiTacchio, Kevin R Hayes, Christopher Vollmers, Satchidananda Pulivarthy, Julie E Baggs, Satchidananda Panda, and John B Hogenesch. 2009. “Harmonics of Circadian Gene Transcription in Mammals.” *PLoS Genetics* 5 (4): e1000442.

Hughes, Michael E, John B Hogenesch, and Karl Kornacker. 2010. “JTK_CYCLE: An Efficient Nonparametric Algorithm for Detecting Rhythmic Components in Genome-Scale Data Sets.” *Journal of Biological Rhythms* 25 (5): 372–80.

Ko, Caroline H, and Joseph S Takahashi. 2006. “Molecular Components of the Mammalian Circadian Clock.” *Human Molecular Genetics* 15 (suppl_2): R271–77.

Levine, Daniel C, Haein Hong, Bridget J Weidemann, Kathryn Moynihan Ramsey, and Joseph Bass. 2020. “Circadian Control of Metabolism and Cancer Risk.” *Cancer Research* 80 (3): 479–86.

Masri, Selma, and Paolo Sassone-Corsi. 2018. “The Emerging Link Between Cancer, Metabolism, and Circadian Rhythms.” *Nature Medicine* 24 (12): 1795–1803.

Matsuo, Takuya, Shigeru Yamaguchi, Shinichi Mitsui, Akio Emi, Fumiyuki Shimoda, and Hitoshi Okamura. 2003. “Control Mechanism of the Circadian Clock for Timing of Cell Division in Vivo.” *Science* 302 (5643): 255–59.

Mure, Ludovic S, Hiep D Le, Giorgia Benegiamo, et al. 2018. “Diurnal Transcriptome Atlas of a Primate Across Major Neural and Peripheral Tissues.” *Science* 359 (6381): eaao0318.

Nguyen, Anna L, Megan A Lausten, and Bruce M Boman. 2025. “The Colonic Crypt: Cellular Dynamics and Signaling Pathways in Homeostasis and Cancer.” *Cells* 14 (18): 1428.

Ogata, Katsuhiko. 2010. *Modern Control Engineering*. 5th ed. Prentice Hall.

Ouyang, Li, Yang Li, Qi Chen, et al. 2024. “Circadian Clock Regulation of Wee1 and Implications for Cancer Chronotherapy.” *Cells* 14 (18): 1428.

Panda, Satchidananda, Marina P Antoch, Brooke H Miller, et al. 2002. “Coordinated Transcription of Key Pathways in the Mouse by the Circadian Clock.” *Cell* 109 (3): 307–20.

Reppert, Steven M, and David R Weaver. 2002. “Coordination of Circadian Timing in Mammals.” *Nature* 418 (6901): 935–41.

Sancar, Aziz, and Russell N Van Gelder. 2021. “Clocks, Cancer, and Chronochemotherapy.” *Science* 371 (6524): eabb0738.

Sims, Christopher A. 1980. “Macroeconomics and Reality.” *Econometrica* 48 (1): 1–48.

Storch, Kai-Florian, Octavian Lipan, Igor Leykin, et al. 2002. “Extensive and Divergent Circadian Gene Expression in Liver and Heart.” *Nature* 417 (6884): 78–83.

Strogatz, Steven H. 2015. *Nonlinear Dynamics and Chaos: With Applications to Physics, Biology, Chemistry, and Engineering*. 2nd ed. Westview Press.

Takahashi, Joseph S. 2017. “Transcriptional Architecture of the Mammalian Circadian Clock.” *Nature Reviews Genetics* 18 (3): 164–79.

Thaben, Paul F, and Pär O Westermark. 2014. “Detecting Rhythms in Time Series with RAIN.” *Journal of Biological Rhythms* 29 (6): 391–400.

Ueda, Hiroki R, Akira Matsumoto, Masahiro Kawamura, et al. 2002. “A Transcription Factor Response Element for Gene Expression During Circadian Night.” *Nature* 418 (6897): 534–39.

Weisel, K, I Mellinghoff, E Halilovic, et al. 2015. “Targeting Wee1 in Cancer Therapy.” *Clinical Cancer Research* 21 (20): 1–7.

Whiteside, Michael. 2026. “AR(2) Eigenvalue Modulus as a Measure of Temporal Persistence in Gene Expression: Circadian Hierarchy Emerges from Two Coefficients.” *bioRxiv*.

Zhang, Ray, Nicholas F Lahens, Heather I Ballance, Michael E Hughes, and John B Hogenesch. 2014. “A Circadian Gene Expression Atlas in Mammals: Implications for Biology and Medicine.” *Proceedings of the National Academy of Sciences* 111 (45): 16219–24.

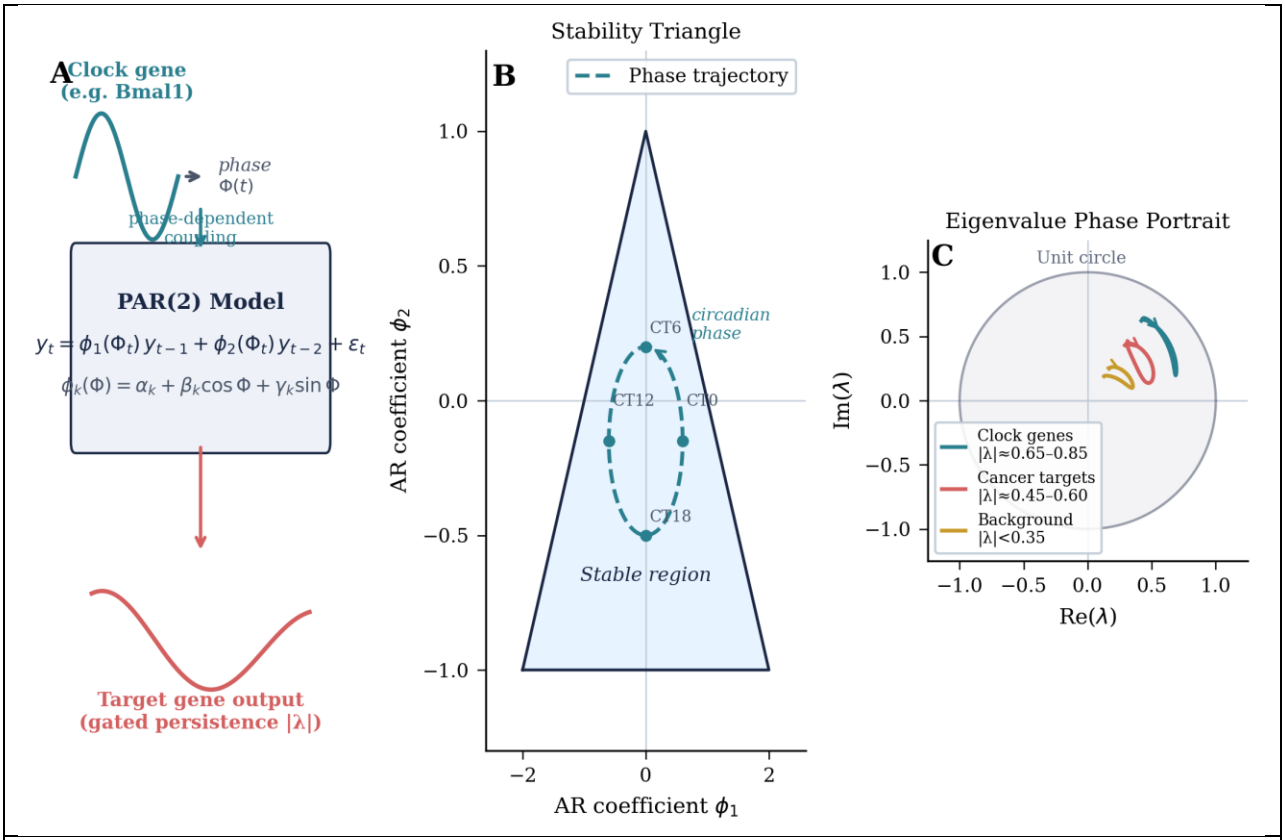



Figure 1

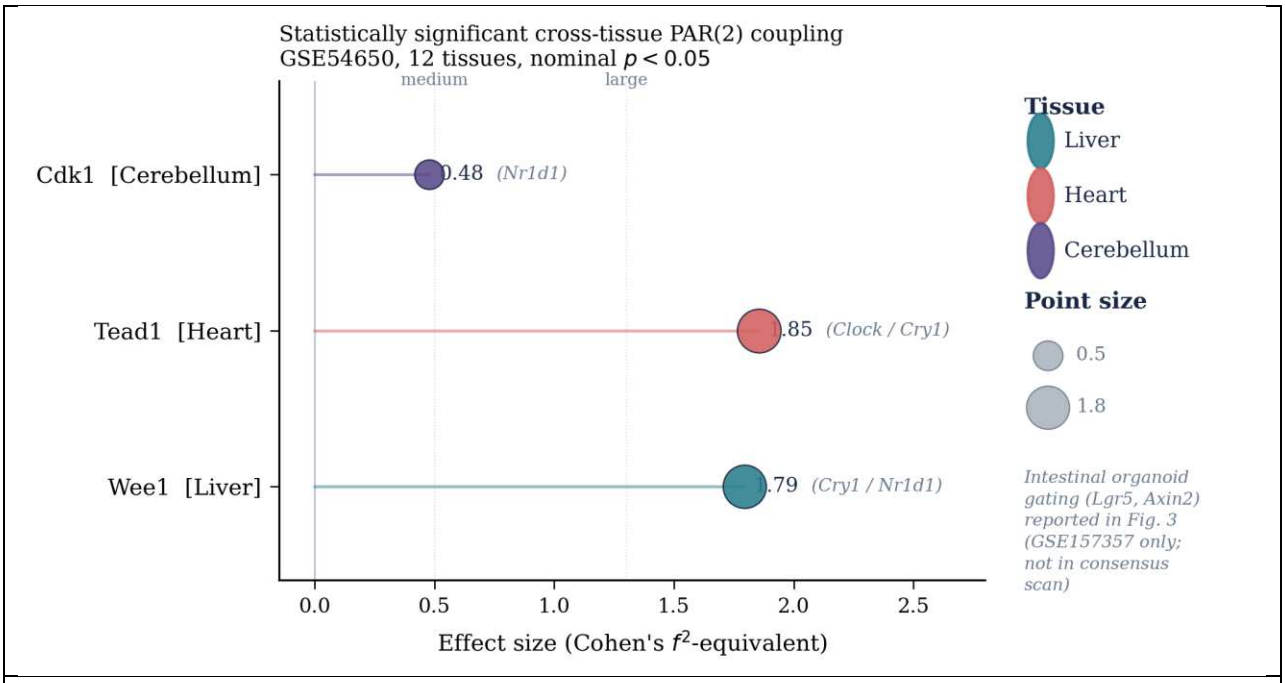



Figure 2

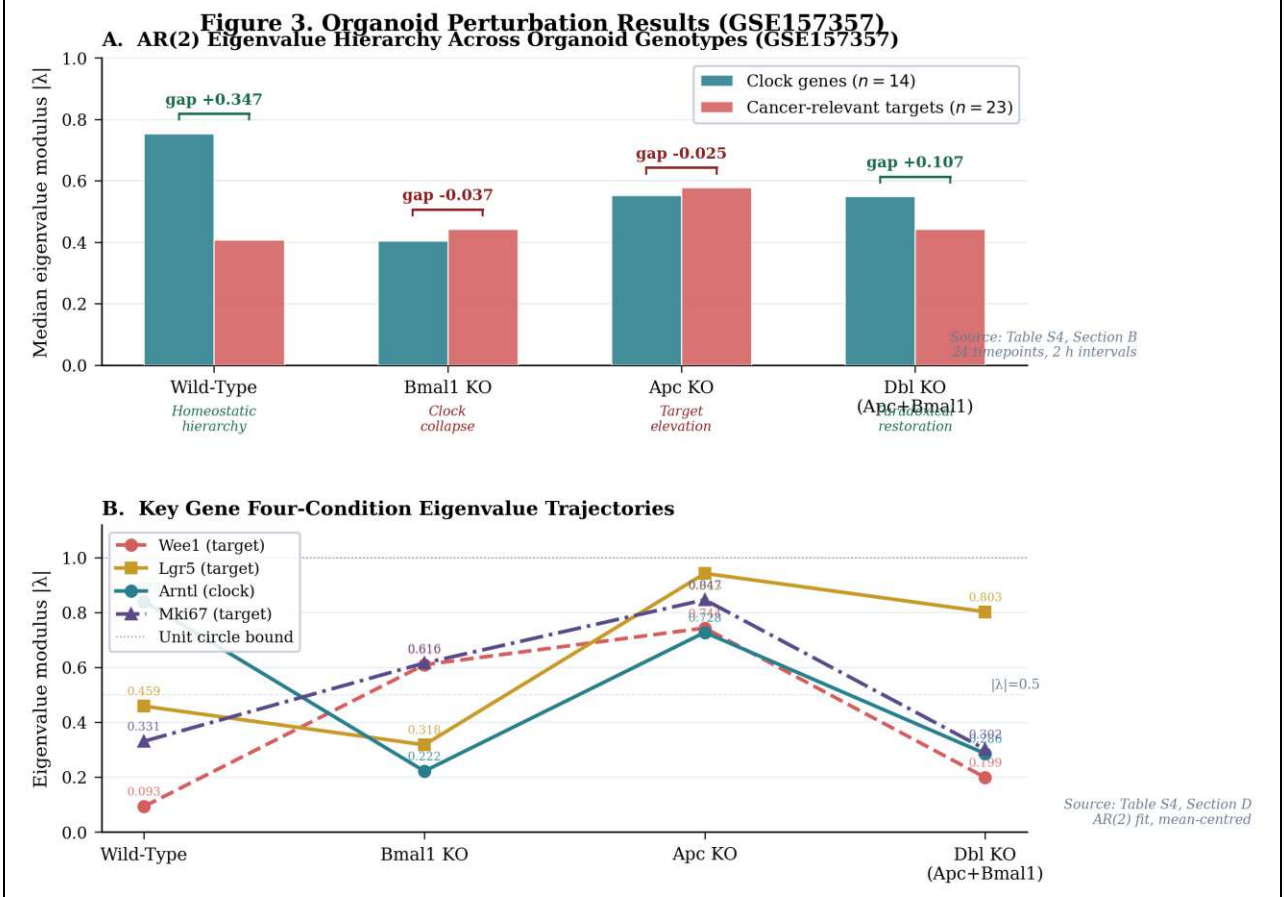



Figure 3

## Supplementary Files

This is a list of supplementary files associated with this preprint. Click to download.

- SupplementaryTableS5EigenvalueSummaries.csv
- SupplementaryTableS5EigenvalueSummaries.csv
- SupplementaryTableS3TieredHits.csv
- SupplementaryTableS2GoldenRatioEnrichment.csv
- SupplementaryTableS2GoldenRatioEnrichment.csv